

University of Ljubljana

Faculty of Mathematics and Physics



Seminar

Magnetic tweezers for DNA manipulation

Ivna Kavre

Adviser: prof. dr. Rudolf Podgornik

Ljubljana, March 2011

Abstract

There are several experimental techniques that allow the mechanical manipulation of a single-molecule and the sensing of its interactions with other biomolecules. The most promising technique for detailed studies of single-molecule manipulation and rotation is the magnetic tweezer. The force measurement consist in measuring the displacement of a small sensor tethered to a fixed surface by a polymer. Recent theoretical developments facilitate performing experiments on the plectoneme formation with DNA and local melting of DNA by twisting it.

Contents

1.Introduction.....	3
2. Single-molecule experimental techniques.....	3
3.Magnetic tweezers.....	5
3.1. Superparamagnetic beads.....	6
3.2. Permanent magnet configuration.....	6
3.3. Magnetic interaction.....	6
4.Manipulation of single-molecule by MT.....	10
4.1.Introduction to DNA.....	10
4.2.Plectoneme formation.....	10
4.3.DNA melting.....	13
5.Conclusion.....	15
Reference.....	16
Figures.....	17

1. Introduction

Single-molecule study has become one of the most popular theme of research in modern biophysics. The history of single-molecule experiments is correlated to the history of single-molecule imaging. We can say that the single-molecule experiments begin with the invention of the optical tweezers and the scanning tunneling microscope.

One of the main goals in the modern biology is to characterize and understand the function of all constituent parts of the living organism, and ultimately, the chemistry of life [1].

Over the past few years, the single-molecule techniques have been used by the biophysicist to study the structure of individual biopolymers such as DNA, RNA and proteins [2]. For example, micromanipulation of single DNA molecule, allows precise study of the proteins which process DNA [3]. With the modern techniques is possible to directly observe and physically characterize fundamental biological processes such as the reading of the DNA sequences, DNA replication, and the activity of enzymes which split the DNA double helix into single strands.

This seminar is focused on the magnetic tweezer technique and the manipulation of single-molecule (DNA molecule) by magnetic tweezers.

2. Single-molecule experimetal techniques

In the past ten years, a variety of experimental techniques have been developed that allow the mechanical manipulation of a single biological molecule and the sensing of its interactions with other biomolecules, such as atomic force microscopy (AFM), laser optical tweezers (LOT), magnetic tweezers (MT),... These single-molecule techniques are very sensitive; they are capable of applying piconewton-scale forces and measuring displacements of nanometers.

On one hand, the working principle of all the mentioned techniques is the same, on the other hand, each technique enables some experiments that are not possible with the others.

In the next few paragraphs, I will briefly try to describe experiment preparation, the principle of working, the drawbacks and the advantages of each technique.

Typically, a DNA molecule, a RNA molecule, a protein or some other polymer is first anchored to a surface with one end and with the other to a probe – through which force is applied. The probe is usually a trapped micron-sized bead (for the LOT, MT) or a tip (in the case of the AFM), the displacement of which allows the measurement of the force [2]. For anchoring the molecule, the surface and the probe have to be prepared in a specific way, as described below. One end of the probe is coated with a chemical substance (avidin or streptavidin), that can bind specifically to its complementary molecule (biotin). For that reason, the molecule of interest (DNA, RNA, protein,...) is coated at one end with biotin molecules, as shown in figure 1. As mentioned before, the molecule of interst has to be anchored at two sides (one of the sides is anchored

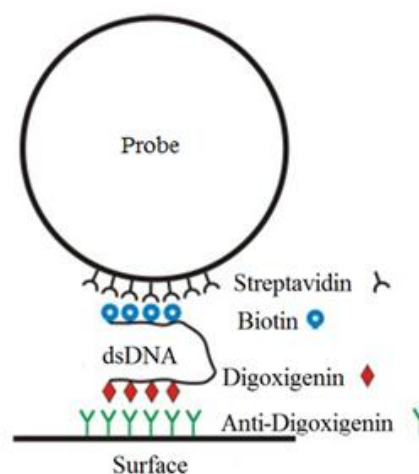


Figure 1. The preparation of the molecule (dsDNA), the surface and the probe before the anchoring.

to a probe, as described). The other side has to be anchored to the surface (as in the case of the AFM and MT), or to another bead on the micropipette (as in the case of the LOT). To avoid double attachment between the two ends of a single molecule and the same bead it is customary to differently label the molecule at its two ends. One end is then labeled with

biotin, the other with digoxigenin. So, the surface (or bead on the micropipette) is then coated with anti-digoxigenin. The described preparation has to be done very carefully, because it is a crucial part for a good experiment.

The techniques such as AFM, LOT and MT are used to manipulate and exert mechanical force on individual molecules. The choice of the probe, which is going to be manipulated, is limited with the choice of the instrumentation. For example, in the AFM the probe is the cantilever's tip (fig. 2A). Dielectric beads can be manipulated with the LOT (fig. 2B), while superparamagnetic beads can be manipulated with the MT (fig. 2C).

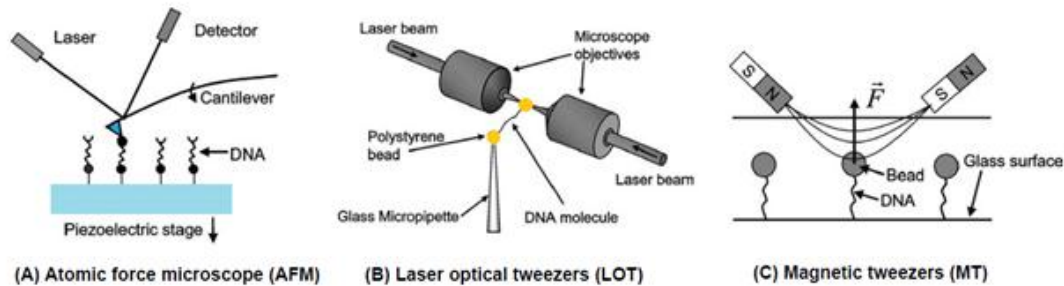


Figure 2. Experimental techniques: (A) Atomic Force Microscope (AFM); (B) Laser Optical Tweezer (LOT); (C) Magnetic Tweezer (MT).

As said before, in all the three techniques, the molecule of interest is attached at two macroscopic bodies. In the AFM, one end of the molecule is attached to the surface (glass surface), which is positioned on the piezoelectric stage, while the other end is attached to the cantilever's tip which deflection is detected by the reflection of a laser beam (fig. 2A).

In the LOT, the molecule is anchored at two dielectric beads. One of the beads is trapped in the optical well whereas the other bead is immobilized on the tip of a micropipette and held fixed by air suction (fig. 2B).

In the MT, a superparamagnetic bead is used as a probe, which is manipulated by an external magnetic field generated by two magnets (fig. 2C).

All the three techniques have in common the determination of molecules extension, which is determined from the position of the probe relative to the surface. The precision and accuracy of the measurements, therefore depend critically on the ability to measure the position of the probe [5].

In the next paragraphs are nominated the drawbacks and the advantages of the three techniques.

Laser optical tweezers allow measurement of piconewton forces and nanometer displacement on the beads attached to one end of the molecule of interest. Although a lot of properties can be nominated that make LOT extremely well suited for the measurement of force and motion, one has also to consider its limitations and drawbacks. Whereas many of the advantages afforded by LOT stem from their purely optical origin, there are some important difficulties associated with using light to generate force:

- as trap stiffness depends on the gradient of the optical field, optical perturbations that affect the intensity or the intensity distribution will degrade the performance of optical tweezers
- any dielectric particle near the focus of the trapping laser will be trapped. For this reason, samples in which the objects that will be trapped are freely diffusing must be kept at extremely low concentration to prevent additional objects from being trapped once the first object is captured
- the application of constant, well-calibrated forces is technically challenging
- the intense laser spot can photodamage the molecule being studied

Although AFM is a very versatile and powerful tool, it has a few drawbacks for manipulating single molecules:

- the presence of undesired interactions between tip and substrate, as the Van der Waals, electrostatic and adhesion forces
- the difficult to control the specific location of the attachment between the tip and the molecule
- the force limitation, i.e. AFM cannot measure forces <10 pN [5].

All in all, AFMs are ideal to investigate strong to covalent interactions. They have been used to probe relatively strong intermolecular and intramolecular interactions (for example, pulling experiments in biopolymers).

LOT and AFM setups also have the disadvantage of being quite expensive.

Despite their many unique features, MT are not nearly as vesatile as LOT or AFM. The robust permanent magnet configuration lack the manipulation ability of other techniques. Because its stiffness is a function of the force, the MT technique is limited at weak forces, <1 pN. Although MT has several drawbacks, it has a lot of advantages compared to AFM or LOT. For example, MT allow simple twisting of the molecule of interese, which is achieved by rotating the magnetic bead in a rotating magnetic field. A further bonus of the MT is that measurements on DNA at constant force are trivial – all you need to do is keep the distance between the magnets and the sample fixed – without the need of feedback (like in the AFM and LOT). Additional advantages include the facile extension to parallel measuremets of multiple molecules, the absence of sample heating and photodamage [6].

Till now, I tried to present the main characteristic of the three most known single-molecule techniques. In the next chapter I am gonig to describe the MT technique in more details.

3. Magnetic tweezers

Magnetic tweezers (MTs) are a single-molecule technique that allow us to manipulate and rotate small bodies or single micromolecules. In a typical configuration a DNA or RNA molecule is anchored with one end to the surface of a flow cell and with the other end to a micron-sized superparamagnetic bead that can be manipulated by means of macroscopic magnetic filed generate by permanent magnets (as shown in fig.3) or electromagnets [6], [7]. The use of electromagnets show some advantages, the main one is the possibility to change the force by changing the current in the coils. One of the disadvantages is its dimension. It is so big that is difficult to move the magnetic circuit. Compared with the electromagnets, permanent magnets allow the construction of compact magnetic circuits, that can be rotated around the vertical axis; this is useful when we want to rotate the bead in order to twist the molecule of interest [8].

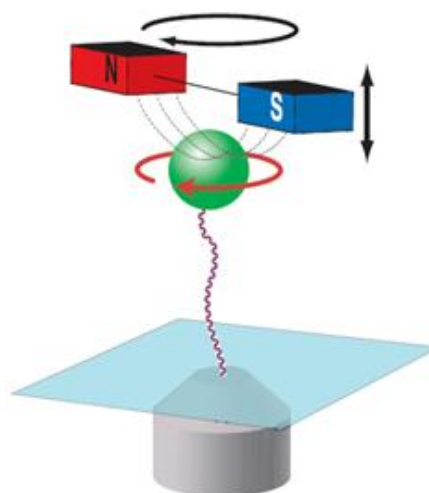


Figure 3. Schematic representation of magnetic tweezers (MTs) with permanent magnets.

In figure 3 is shown a schematic representation of MTs with permanent magnets. A superparamagnetic bead (green) is anchored to the surface of the trapping chamber by a single

molecule of DNA. The magnetic field gradient (dashed lines) along the axial direction, is produced by a pair of small permanent magnets (red and blue) which are positioned above the trapping chamber. The magnetic field gradient results in a force on the bead directed up toward the magnets. By moving the magnets in the axial direction (bidirectional arrow), one can control the force. By rotating the magnets (black circular arrow), one can rotate the magnetic bead (red circular arrow). So, as mentioned before, a MT is a technique that enable the manipulation and the rotation of the molecule of interest [5].

3.1. Superparamagnetic beads

Superparamagnetic beads are used in a MTs' probe. The probe size goes from 0.5 μm to 5 μm [5]. In most of the cases the beads are composed of $\sim 10\text{-}20$ nm magnetic particles embedded in a porous matrix sphere enclosed in a protective polymer shell. If there is no external magnetic field, the magnetic domains are thermally disordered, and there is no residual magnetization, which prevents aggregation. If the beads are collocate in an external magnetic field, it orients the magnetic domains. The result is a large magnetic moment aligned with the magnetic field. The rate of magnetization decay is governed by the Néel-Arrhenius equation.

External magnetic field \mathbf{B} aligns the dipole moments of superparamagnetic particles and thus induces magnetic dipole moment \mathbf{m} in the particle. The induced dipole moment is proportional to \mathbf{B} for small magnetic fields:

$$\mathbf{m} = \chi V \frac{\mathbf{B}}{\mu_0} \quad (1)$$

where V is the volume of the bead, χ is the magnetic susceptibility of the particle and $\mu_0 = 4\pi \times 10^{-7} \text{Vs/Am}$ is the inductance constant.

As said before, one of the advantages of the MT is the rotation of the molecule of interest. That can be done, anchoring the molecule to the bead. Rotating the external magnetic field results in bead rotation and therefore in molecule rotation.

3.2. Permanent magnet configuration

Typically the magnetic field in the MT is generated by a pair of permanent rare earth magnets. The strongest available permanent magnets are the neodymium iron boron ($\text{Nd}_2\text{Fe}_{14}\text{B}$) magnets, also called NIB or neodymium magnets [5]. The magnets are small, about a few millimeters. They are collocated in such a way that the north pole of one magnet faces the south pole of the other one, separated by a ~ 1 mm gap. The magnetic field strength decrease roughly exponentially with a characteristic length scale comparable to the separation between the magnets. The force on the magnetic particle changes in proportion to displacement. One of the disadvantages of MT based on permanent magnets is the impossibility of manipulation the magnetic particle in three dimensions. On the other hand, that kind of MT are well-suited for constant force experiments.

3.3. Magnetic interaction

The energy of a superparamagnetic particle in a magnetic field \mathbf{B} is given by:

$$U = -\mathbf{m}(\mathbf{B}) \cdot \mathbf{B} \quad (2)$$

where $\mathbf{m}(\mathbf{B})$ is the magnetic moment of the particle, which is in turn dependent on the external field. The force experienced by the particle is given by the negative gradient of the energy

$$\mathbf{F} = -\nabla U = \nabla(\mathbf{m}(\mathbf{B}) \cdot \mathbf{B}) \quad (3)$$

For small external fields, the magnetic moment is linear in the external field (eq.1). In this case, the force is proportional to the gradient of the square of the magnetic field

$$\mathbf{F} = \frac{V\chi}{\mu_0} \nabla |\mathbf{B}|^2 \quad (4)$$

For large fields, the magnetic moment of the beads reaches the saturation value \mathbf{m}_{sat} and the force is proportional to the gradient of the magnetic field

$$\mathbf{F} = \nabla(\mathbf{m}_{\text{sat}} \cdot \mathbf{B}) \quad (5)$$

One of the possibility to exert a magnetic force is to use a combination of a homogeneous magnetic field and superparamagnetic particles. The device cannot exert a force on a single isolated particle but rather a force acts between induced magnetic dipoles in the particles. Either repulsive or attractive forces can be induced by proper modulation of the amplitude and direction of the magnetic field [8].

All single-molecule force measurement techniques consist in measuring the displacement of a small sensor (bead or AFM cantilever) tethered to a fixed surface by a polymer (DNA, RNA, protein,...). This system is equivalent to an inverted dumped pendulum (fig. 4) [2].

Two ways of MT calibration in flow fields can be nominated; the one using Stokes' law the other one measuring Brownian motion.

C. Haber and D. Wirtz, as S.B. Smith et al. propose the MT calibration using Stokes' law. Haber and Wirtz [9] measured the magnetic force on untethered magnetic beads, suspended in a medium containing CaCl_2 using a balance between the applied magnetic force and the resulting friction force on the beads. Since the Reynolds number did not exceed 10^{-5} , Stokes' law can be used. Thus, the force applied on the magnetic bead can be estimated:

$$F \approx 6\pi\eta a v \quad (6)$$

where η is the buffer viscosity, a the bead radius and v the measured bead velocity.

For Smith et al. [10], the application of Stokes' law was justified by low Reynolds number ($\sim 10^{-3}$).

On the other hand, R. Seidel and D. Klaue [4], as T.R. Strick at al. [2], [11] propose the MT calibration measuring Brownian motion as described below. Suppose to produce a force along the z axis. The analysis of the horizontal Brownian motion of the particles permits measurement of the stretching force. It is simple to imagine: as harder the magnetic force is pulling the bead as harder is it for the bead to leave the upright stretching position and as small is the Brownian motion. The bead-positioning software determines the DNA extension l (which correspond to the pendulum's length) and the particle transverse fluctuations δx [12]. A restoring force (F_b), which is proportional to small displacements, tends to bring the bead back to equilibrium. It can be compared to a spring with a spring constant κ , which is in this case F/l . According to the equipartition theorem, the mean energy of the spring ($E = \frac{1}{2}\kappa\langle x^2 \rangle$) in one dimension is equal to the thermal energy per degree of freedom, which is $\frac{1}{2}k_B T$. In that way, one obtain the formula which connect the pulling force (F), with the length of the DNA molecule (l) and the mean square displacement in x ($\langle x^2 \rangle$):

$$F = \frac{k_B T l}{\langle x^2 \rangle} \quad (7)$$

In this approach, one can encounter some problems. The »pendulum« is subjected to continuous thermal shocks that limit the accuracy of force/displacement measurement. By the fluctuation-dissipation theorem the Langevin force noise δf_n is related to the dissipation

$$\delta f_n = \sqrt{4k_B T \gamma \Delta f} \quad (8)$$

where $\gamma = 6\pi\eta r$ is the viscous dissipation and Δf the measurement frequency bandwidth.

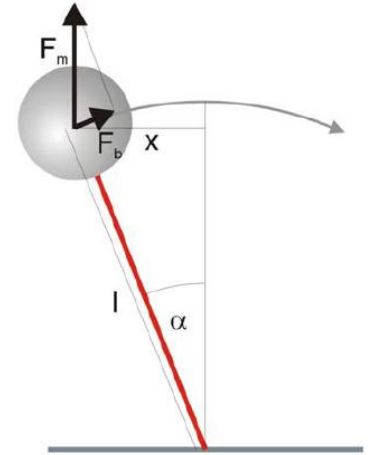


Figure 4. The magnetic force acting on a bead can be obtained by the analysis of the horizontal Brownian motion and applying the equipartition theorem.

In a force clamp configuration such as obtained with a MT, the force is fixed and the molecule's extension is measured.

In the next part of this chapter will be presented some results of J. Lipfer, X. Hao and N.H. Dekker [6]. They have computed the magnetic fields from pairs of permanent magnets in two distinct orientations: the vertical and the horizontal orientation (fig. 5). In the vertical orientation the magnets' moments are antiparallel and point toward and away from the flow cell, while in the horizontal orientation the magnetic moments are aligned, parallel to the surface of the flow cell (fig. 6).

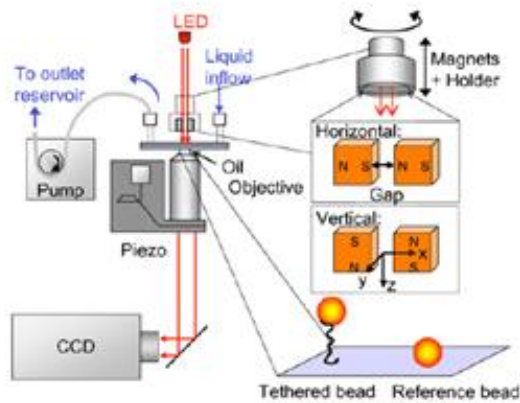


Figure 5. Schematic representation of the basic component of the MT setup: the inverted microscope, the CCD camera, the flow cell system with in- and outlet and the LED illumination. On the right side is shown the zoom-in of the flow cell with a tethered and a reference bead and the magnet pairs in horizontal and vertical geometry.

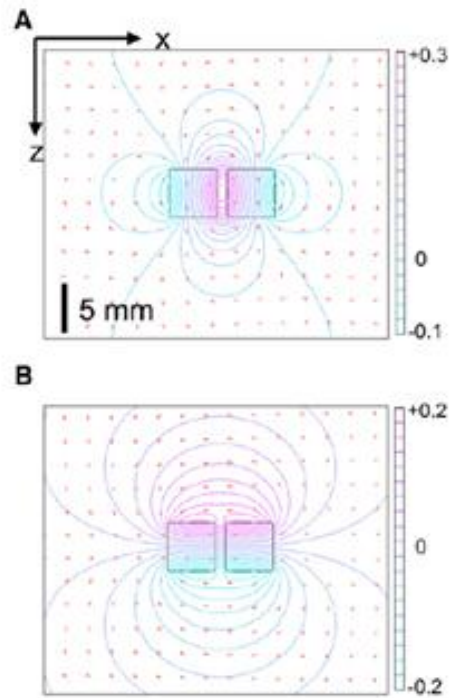


Figure 6. Simulation of magnets in vertical (A) and horizontal (B) configuration. Graphs show color-coded iso-contour lines of the z component of the magnetic vector potential A_z .

Beside the magnet shape (in [6] are used cubic magnets of size $5 \times 5 \times 5$ mm) an important parameter of the magnet geometry is the gap, i.e. the distance between the magnets. In the two graphs that follows (fig. 7A, 7B) are shown the magnetic fields measured and computed along the z axis (fig. 5) for pairs of magnets in vertical (brown and red symbols) and horizontal (light and dark blue symbols) configuration. As said, another important parameter is the gap g , and it has also been taken in consideration. Figure 7A shows data for $g = 1$ mm and 7B shows data for $g = 2$ mm. Data points are from measurements in the absence (red and light blue) and presence (brown and dark blue) of an iron yoke. The black dashed lines correspond to the magnetic field computed from the semianalytical theory.

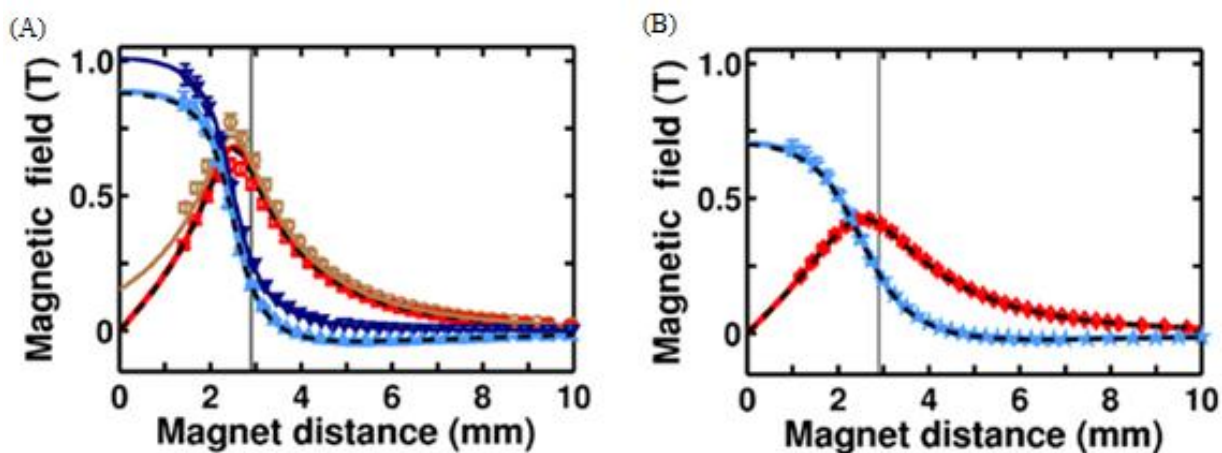


Figure 7. Magnetic field vs. magnetic distance curves for pairs of permanent magnets; (A) $g = 1$ mm, (B) $g = 2$ mm.

Knowing the magnetic field, one can compute the force exerted on tethered superparamagnetic particles using equation 1. In the next two graphs (fig 8) are shown the magnetic forces for tethered superparamagnetic beads in comparison to the magnetic distance. The symbols and colors of the lines are the same as in figures 7. The graphs show the forces as a function of magnet position for $g = 1$ mm (fig. 8A) and $g = 2$ mm (fig. 8B). Positive values correspond to forces that pull the beads away from the flow cell surface, toward the magnets. The shaded region represents the region that is experimentally inaccessible due to the finite thickness of the flow cell.

The mentioned geometry, i.e. two permanent magnets in the horizontal and vertical configuration, are the most used configurations. They provide the robust and straight forward handling of samples and permit one to apply torque to the tethered beads. However, other magnet geometries are possible. Every geometry has some advantages but also disadvantages. So, the choice of the geometry depends on what are we going to measure.

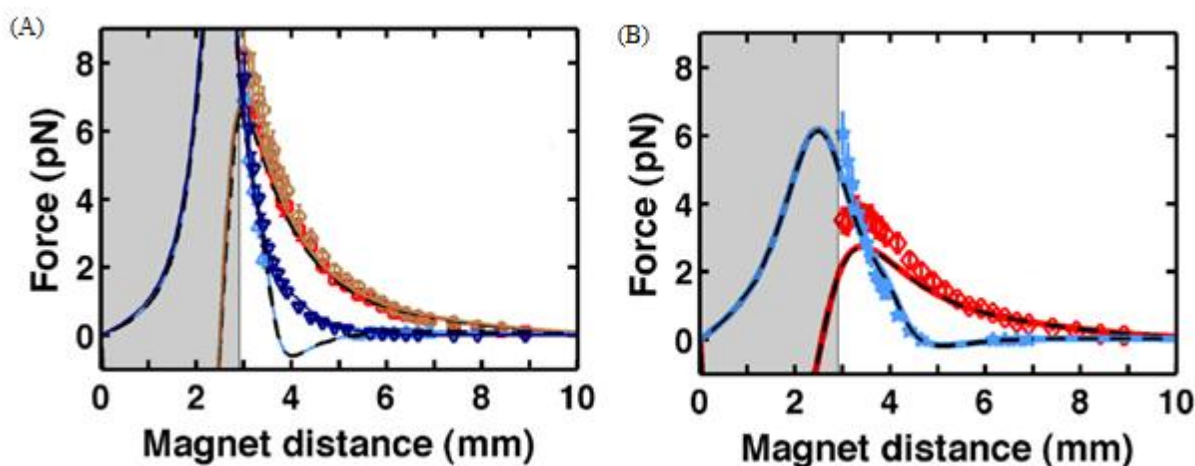


Figure 8: Force vs. magnet distance curves for pairs of permanent magnets; (A) $g = 1$ mm, (B) $g = 2$ mm

4. Manipulation of single-molecule with MT

Magnetic tweezers are single-molecule manipulation instrument that utilize a magnetic field to apply force to a biomolecule tethered magnetic bead. Till now, I presented the experimental techniques that may be used to single-molecule study, their advantages and disadvantages, the principle of working and the physical background of the magnetic tweezers. Now, I am going to introduce the DNA molecule and to present some results obtained studying the plectoneme formation and the DNA melting by twisting it.

4.1. Introduction to DNA

DNA, or deoxyribonucleic acid is a nucleic acid that contains the genetic instructions used in the development and functioning of all known living organisms. The information in DNA is stored as a code made up of four bases: adenine (A), guanine (G), cytosine (C), and thymine (T). DNA bases pair up with each other, adenine with thymine, and cytosine with guanine, to form units called based pairs. Each base is attached to a sugar molecule and a phosphate molecule. Together, a base, sugar, and phosphate are called a nucleotide. Nucleotides are arranged in two long strands that form a spiral called a double helix (fig. 9).

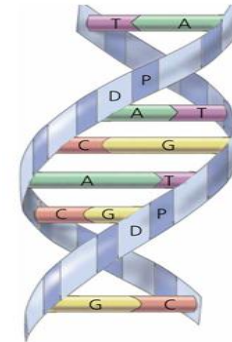


Figure 9. Schematic representation of a DNA molecule.

An important property of DNA is that it can replicate, or make copies of itself. Each strand of DNA in the double helix can serve as a pattern for duplicating the sequence of bases.

In the next chapter will be presented the formation of plectonemes and will be introduced a topological formalism used to study DNA twisting.

4.2. Plectoneme formation

Vinograd first understood in 1965 that the double-helical nature of DNA allows it to be overwound and unwound from its natural state [11]. On a twisted phone cord one often notice the formation of interwound structures, called plectonemes (from the Greek meaning »braided string«), which appear to be a way of releasing torsional stress.

Formation of plectonemes in filaments can be observed in yarn, hair, strands, garden hoses and telephone or computer cords. The process of plectoneme formation is easily demonstrated by holding a string or wire taut by exerting forces at its ends, twisting it and then relieving the tension [15].

The MT techniques gives us the possibility of stretching (fig. 10A) or twisting (fig. 10B) the DNA molecule.

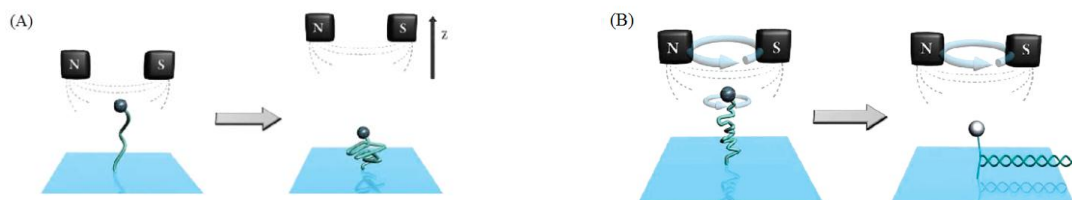


Figure 10. Schematic sketch of the MT technique. (A) shows the stretching of the DNA molecule. When the magnet is lowered, the force becomes stronger and the DNA is highly stretched by the magnetic force acting on the bead. (B) shows the twisting of the DNA molecule and the formation of plectonemes. By rotating the external magnets at a fixed height, the MT technique creates the possibility of applying a torque to torsionally constrained DNA.

Before analyzing the plectoneme formation, a topological formalism used to study DNA twisting must be presented. In function of that few simple quantities should be mentioned (fig.11):

- Twist (Tw) of the molecule – the number of times the two strands that make up the double helix twist around each other (typically is one turn over 10.4-10.5 base pairs) [1], [2], [7], [11] [16], [17]
- Writhe (Wr) of the molecule – the number of times the axis of the molecule crosses itself

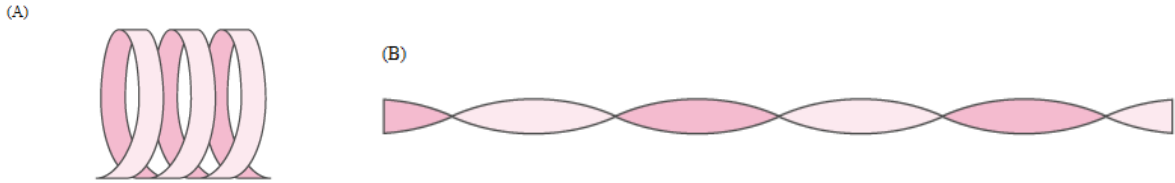


Figure 11. Representation of writhe and twist. (A) shows large writhe and small change in twist, (B) shows zero writhe and large change in twist.

If one constrains the end of the DNA molecule, then the total number of times that the two strands of the helix cross each other (either by twist or by writhe) becomes a topological invariant of the system known as the linking number, Lk .

A mathematical theorem due to White (1969) states that:

$$Lk = Tw + Wr = const \quad (9)$$

While a linear DNA molecule, in the absence of external constraints, has neither writhe nor macroscopic curvature, we can write $Wr = 0$. Thus, the natural linking number Lk_0 is equal to the number of helical turns of the molecule $Lk_0 = Tw_0$.

When $Lk \neq Lk_0$, we say that the molecule is supercoiled, i.e. the molecule has an excess or a deficit of linking number relative to its torsionally relaxed state. Thus, we can define the excess linking number (or degree of supercoiling) σ :

$$\sigma = \frac{Lk - Lk_0}{Lk_0} \quad (10)$$

When $\sigma > 0$ the molecule is overwound, when $\sigma < 0$ the molecule is unwound.

For understanding the elastic behaviour of coiled DNA we can use an analogy with twisting a rubber tube under an applied force F , as shown in figure 12A. Upon twisting the system, it takes a number of turns before the tube length reduces significantly and plectonemes are formed.

Rotating the bead attached to a torsionally constrained DNA molecule changes its linking number Lk . If we start from a torsionally relaxed molecule, the change in linking number is absorbed by elastic twist deformations and increases twist Tw of the molecule, while the writhe Wr remains unchanged. In this regime, the torque Γ increases linearly with the twist angle $\Omega = 2\pi n$ (which increases linearly with the number of turns n),

$$\Gamma = \frac{C}{l_0} \Omega = 2\pi n \frac{C}{l_0} \quad (11)$$

where C is the torsional stiffness, ($C = 90k_B T$ for DNA) and l_0 is the length of the DNA.

The twist energy increases quadratically:

$$E_{\text{torsion}} = \frac{1}{2} \frac{C}{l_0} \Omega^2 \quad (12)$$

As said before, after a certain number of turns n_b (corresponding to a torque $\Gamma_b = \frac{2\pi n_b C}{l_0}$) the system undergoes a buckling transition where the additional mechanical energy is no longer stored as an elastic twisting deformation but rather in a loop of radius R . As a consequence of loop formation, we can observe a decrease in the extension of the system [19].

The point n_b where the tube (DNA) starts to form plectonemes with a constant reduction per turn is called buckling instability (shown in figure 12A). Up to that point, the torque builds up linearly with the number of turns (fig. 12B). As can be seen in figure 12B, further rotations beyond the buckling instability do not increase T_w , and the torque remains constant. Instead W_r increase as plectonemic supercoils are formed, further decreasing end-to-end distance of the system in a linear fashion [2].

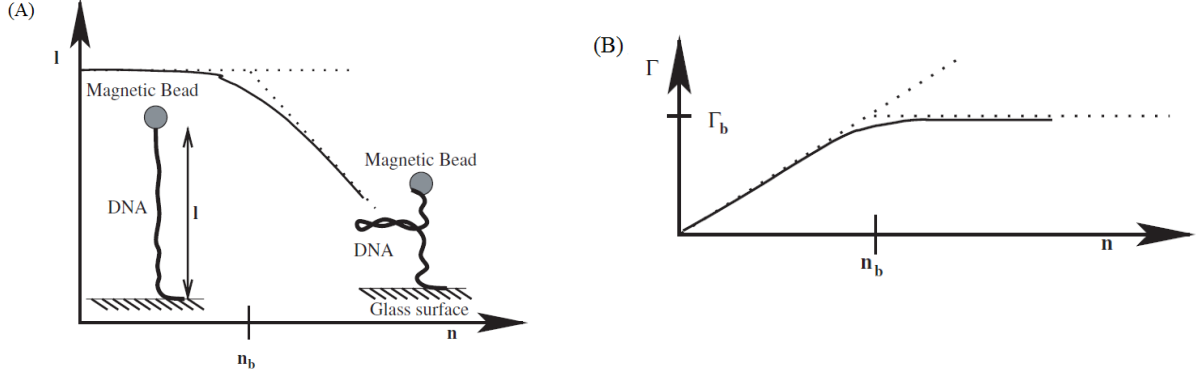


Figure 12. (A) The extension l of an elastic tube which has been stretched and overwound by n turns. (B) Torque Γ acting on the tube as a function of the number of turns n .

Balancing the torsional energy against the work done and the increase in bending energy, we get the following equation:

$$2\pi\Gamma_b = 2\pi R F + 2\pi R \frac{1}{2} \frac{B}{R^2} \quad (13)$$

From eq.13, we can get the critical torque (Γ_b) where plectonemes starts to form:

$$\Gamma_b = \sqrt{2BF} = \sqrt{2l_0 k_B T F} \quad (14)$$

The decrease in the length of the system per turn is:

$$\Delta z = \pi \sqrt{\frac{2l_0 k_B T}{F}} \quad (15)$$

This implies that as the stretching force increases the number of turns required for buckling, n_b , increases and the radius of the tubes coil (plectonemes) after buckling decreases [2].

This model describes very well the behaviour of supercoiled DNA, as can be seen in figure 13. The graph is the result of Stricks' et al. experiments. It shows the curve obtained by overwinding DNA subjected to a stretching force of 1 pN. From the graph, we can identify two regions:

- $n < n_b \sim 140$ - the DNA extension is almost unchanged
- $n > n_b$ - the DNA extension decreases regularly

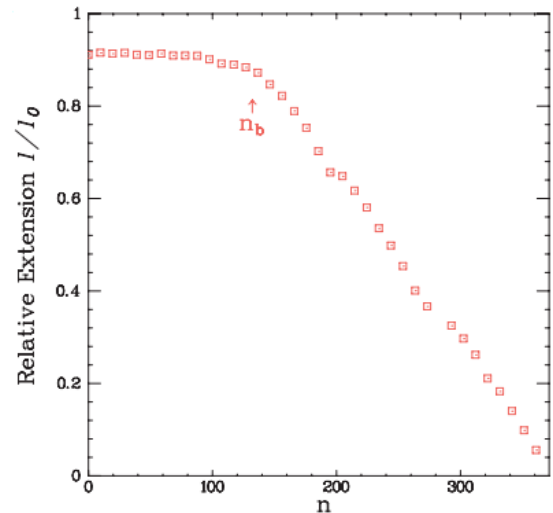


Figure 13. Buckling instability observed on overwound DNA at $F = 1$ pN.

So, inducing plectonemes (at a certain force) reduce the DNA end-to-end distance (fig. 14). Salerno et al. [7] show that at low forces plectonemes are induced independent whether overwinding or unwinding DNA, i.e. the extension versus turns data are symmetric. Specifically, at low force values, we can distinguish two different regions: a central »low turn« region, where the extension is basically constant, and two lateral »high turn« regions where the extension is linearly dependent on the number of turns n .

On the other hand, at slightly higher forces overwinding or unwinding the molecule induce different behaviours due to the intrinsically chiral nature of DNA. At this forces, unwinding generates denaturation bubbles along the DNA [4].

At even higher forces ($F > 5$ pN) one cannot anymore induce plectonemes overwinding the DNA, as it undergoes a structural transition, where the bases start to turn outside and a new hypertwisted DNA structure is generated. In that case, the force versus extension behaviour is similar to that of a torsion-free DNA [11]. So, we can say that at higher forces we denature the DNA molecule. Some words on that topic are spend in the next chapter.

4.3.DNA Melting

This chapter is dedicated to the DNA denaturation. The term »DNA denaturation« refers to the melting of the double-stranded DNA to generate two single strands. This involves the breacking of hydrogen bonds between the bases in the duplex. The most important contribution to DNA helix stability is the stacking of the bases on top of one another. Thus, in order to denature DNA, the main obstacle to overcome is the stacking energies that provide cohesion between adjacent base pairs.

We can nominate at least two major biological reasons for denaturing the DNA within a cell: DNA replication and transcription. In both cases, proteins bind to specific DNA sequences, strongly bend the DNA helix, and then use the localization of torque to force the double-stranded DNA to open (denature – melt) at a specific point.

There are variety of ways in which to denature DNA:

- The most common is heating the DNA to a temperature above its melting point
- Organic solvents as dimethyl sulfoxide and formamide, or high pH, disrupt the hydrogen bonding between DNA strands
- Lowering the salt concentration of the DNA solution aids denaturation by removing the ions that shield the negative charges on the two strands from one another
- Unwinding a DNA molecule (fig. 14)

As mentioned, there are many ways to denature DNA. Since this seminar is focused on the magnetic tweezer and its application in single-molecule manipulation, I will study the DNA denaturation by twisting it.

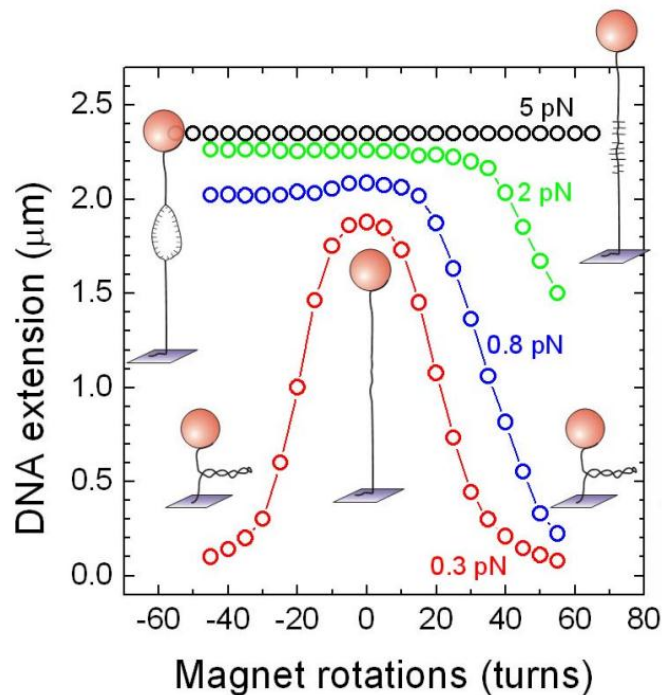


Figure 14. Rotation extension curves for different forces. At higher forces one cannot induce plectonemes but rather denature the DNA molecule.

As shown in figure 14, when unwinding a DNA molecule at forces $F > 5$ pN (by Strick and co-workers), the buckling instability is not observed. While unwinding DNA, its extension varies a little, i.e. the molecule locally denatures rather than forming plectonemes. The denaturation correspond to the two strand unpairing by about 10.5. bases for every extra turn of unwinding [2]. Since White's theorem must be satisfied (eq. 9) writhe is transferred into twist.

As the twist is increased there is a point where it becomes energetically more favorable for the molecule to denature locally and partially relax its twist. This denaturation corresponds to the formation of a small bubble, along which the two constituent strands no longer wrap around each other. As denaturation implies a separation of the two strands, the linking number of this bubble is zero. Thus the formation of a denaturation bubble allows for a small region of the molecule to absorb a large part of the DNA's linking number deficit.

Similarly, overwinding a DNA molecule can induce its local modification assuming that the excess linking number is concentrated into regions of hypercoiled DNA, with the overwound phosphate backbone inside and the unpaired bases exposed on the outside.

Strick et al. estimated the free energy of denaturation using the force versus extension measurements on supercoiled DNA. They considered the case where DNA is twisted at low force by $n = \pm 90$ turns to state A^+ (fig. 15A) requiring a twist energy T_{A^+} . The molecule is then extended to state B^+ so as to pull out its plectonemes and eliminate its writhe. The work performed is $W_{A^+B^+}$. State B^+ could have been reached first by stretching the molecule, at a cost W_{AB} and then twisting it by 90 turns, requiring twist energy T_{B^+} . The mechanical work performed on the molecule by stretching it from thermodynamic state A^+ to B^+ along these two different paths should be equal, thus

$$T_{A^+} = T_{B^+} - \Delta W_{AB^+} \quad (16)$$

where $\Delta W_{AB^+} = W_{A^+B^+} - W_{AB}$.

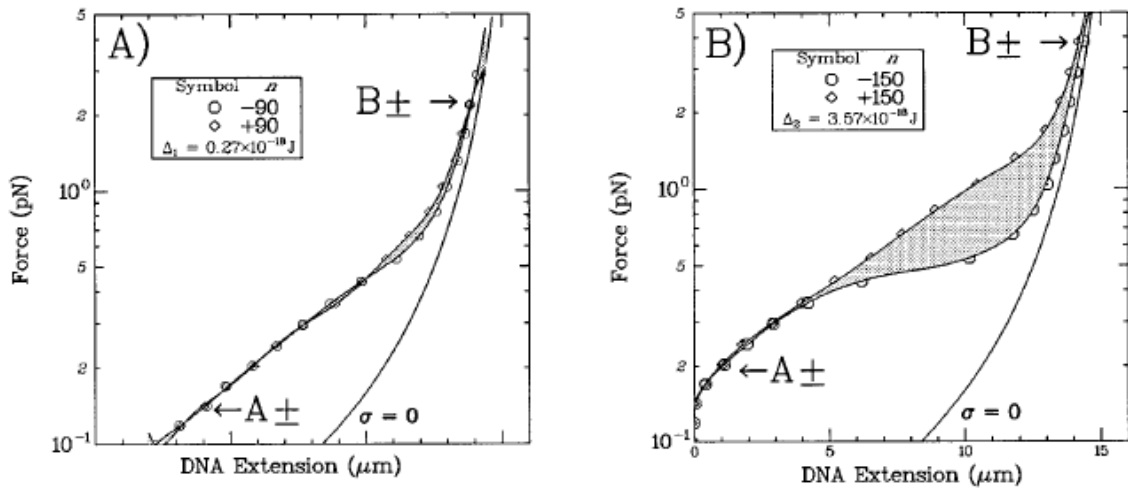


Figure 15. Estimating the energy of denaturation of DNA. (A): \circ , DNA unwound by $n = -90$ turns; \diamond , DNA overwound by $n = 90$ turns. The shaded surface between the σ_+ and σ_- curves represents the work Δ_1 . (B): \circ DNA unwound by $n = -150$ turns; \diamond , DNA overwound by $n = 150$ turns. The shaded surface between the σ_+ and σ_- curves represents the work Δ_2 .

Similarly, for twisting a DNA by $n = -90$, one get $T_{A^-} = T_{B^-} - \Delta W_{AB^-}$. When unwound, the molecule partially denatures as it is pulled from A^- to B^- , thus the torsional energy T_{B^-} will consist of twist energy (E_c - obtained by twisting the DNA by n_c times) and energy of denaturation (E_{d1}), $T_{B^-} = E_c + E_{d1}$. Thus, we got

$$T_{A^-} = E_c + E_{d1} - \Delta W_{AB^-} \quad (17)$$

In the low extension state A^- , the molecule has torsional energy $T_{A^-} = T_{A^+}$.

From equations 16 and 17 one get

$$T_{B^+} - \Delta W_{AB^+} = E_c + E_{d1} - \Delta W_{AB^-} \quad (18)$$

Equation 18 can be written as $E_c + E_{d1} = T_{B^+} - \Delta_1$, where $\Delta_1 = \Delta W_{AB^+} - \Delta W_{AB^-}$

T_{B^+} is the energy of a rod with torsion constant C twisted by n_1 turns

$$E_{d1} + \frac{k_B T}{2} \frac{C}{l_0} (2\pi n_c)^2 = \frac{k_B T}{2} \frac{C}{l_0} (2\pi n_1)^2 - \Delta_1 \quad (19)$$

where $n_1 = n_{d1} + n_c$, k_B is the Boltzmann constant, T the temperature and C the DNA's torsional stiffness.

If the same experiment is performed (fig.15B), changing just the number of turns (not more $n = \pm 90$, but $n = \pm 150$), one can eliminate the part of energy obtained by twisting the DNA n_c times, i.e. E_c . The same type of equation can be written:

$$E_{d2} + E_c = T_{B^+} - \Delta_2 \quad (20)$$

where E_{d2} is the energy of denaturation for $n_2 = n_{d2} + n_c$ turns and Δ_2 is the surface between the curves A^+B^+ and A^-B^- for $n = \pm 150$

Subtracting the equation 20 from equation 19 E_c is eliminated and it yields:

$$E_{d2} - E_{d1} = 2\pi^2 k_B T \frac{C}{l_0} (n_2^2 - n_1^2) - (\Delta_2 - \Delta_1) \quad (21)$$

Finally, the difference $E_{d2} - E_{d1}$ corresponds to the energy involved in converting $n_2 - n_1$ supercoils into a denaturation bubble.

5. Conclusion

There are several experimental approaches for single-molecule manipulation. In this seminar is described in more details the magnetic tweezer (MT). Compared to the other experimental techniques such as atomic force measurement (AFM) and laser optical tweezer (LOT), MT has several drawbacks, but also some advantages. Maybe, one of the main advantages, in comparison with AFM and LOT, is that MT allows simple twisting of the molecule of interest, which is achieved by rotating the magnetic bead in a rotating magnetic field.

Here are presented some experiments on the plactoneme formation with DNA and local melting of DNA by twisting it. At a low force ($F \sim 0.3$ pN) the elastic behaviour of DNA is symmetric whether unwinding or overwinding. The DNA's length decreases and plectonemes are formed. At slightly higher forces ($F \sim 1$ pN), unwinding and overwinding induce different behaviours due to the intrinsically chiral nature of DNA. At this forces, unwinding generates denaturation bubbles along the DNA. At even higher forces ($F \sim 5$ pN), overwinding a DNA molecule generates a new, locally hypertwisted DNA structure.

References

- [1] F. Ritort; Single-molecule experiments in biological physics: methods and applications;
- [2] T.R. Strick, M-N. Dessimges, N.H Dekker, J-F. Allemand, D. Bensimon, V. Croquette; Stretching of macromolecules and proteins; *Reports on Progress in Physics* 66: 1-45, 2003
- [3] J. Yan, D. Skoko, J.F. Marko; Near-field-magnetic-tweezer manipulation of single DNA molecules; *Physical Review E* 70: 011905, 2004
- [4] Handout for Practical Course – Magnetic tweezers and its application to DNA mechanics, tutors: R. Seidel, D. Klaue, Technische Universität Dresden [Online]. (cited on 4th March 2011; 12:08). Available on the internet address http://www.biotech.tu-dresden.de/cms/fileadmin/research/biophysics/practical_handouts/magnetictweezers.pdf
- [5] K.C. Neuman, A. Nagy; Single-molecule force spectroscopy: optical tweezers, magnetic tweezers and atomic force microscopy; *Nature Methods*, vol.5, no.6: 491-504, 2008
- [6] J. Lipfert, X. Hao, N.H. Dekker; Quantitative Modeling and Optimization of Magnetic Tweezers; *Biophysical Journal* 96: 5040-5049; 2009
- [7] D. Salerno, D. Brogioli, V. Cassina, D. Turchi, G.L. Beretta, D. Seruggia, R. Ziano, F. Zunino, F. Mantegazza; Magnetic tweezers measurements of the nanomechanical properties of DNA in the presence of drugs; *Nucleic Acids Research*, vol.38, no.20: 7089-7099, 2010
- [8] N. Osterman, Study of viscoelastic properties, interparticle potentials and self-ordering in soft matter with magneto-optical tweezers (doctoral thesis), University of Ljubljana, Faculty of mathematics and physics, Department of physics, Ljubljana, 2009
- [9] C. Haber, D. Wirtz; Magnetic tweezers for DNA micromanipulation, *Review of Scientific Instruments*, vol. 71, no. 12: 4561-4570, 2000
- [10] S.B. Smith, L. Finzi, C. Bustamante; Direct Mechanical Measurement of the Elasticity of Single DNA Molecules by Using Magnetic Beads, *Science*, vol. 258, no. 5085: 1122-1126, 1992
- [11] T.R. Strick, J.-F. Allemand, D. Bensimon, V. Croquette; Behavior of Supercoiled DNA; *Biophysical Journal*, 74: 2016-2028, 1998
- [12] C. Gosse, V. Croquette; Magnetic Tweezers: Micromanipulation and Force Measurement at the Molecular Level; *Biophysical Journal*, 82; 3314-3329, 2002
- [13] M. Kruihof, F. Chien, M. De Jager, J. Van Noort; Subpiconewton Dynamic Force Spectroscopy Using Magnetic Tweezers; *Biophysical Journal*, 94: 2343-2348, 2008
- [14] Online figure - (cited on 14th March 2011; 11:17). Available on the internet address <http://www.yourdictionary.com/dna>
- [15] P.K. Purohit; Plectoneme formation in twisted fluctuating rods; *Journal of the Mechanics and Physics of Solids*, vol. 56, issue 5: 1715-1729, 2007
- [16] A. Sarkar, J.-F. Leger, D. Chatenay, J.F. Marko; Structural transitions in DNA driven by external force and torque: *Physical Review E*, vol. 63, 051903, 2001

- [17] Z. Bryant, M.D. Stone, J. Gore, S.B. Smith, N.R. Cozzarelli, C. Bustamante; Structural transitions and elasticity from torque measurement on DNA; *Nature*, vol. 424: 338-341, 2003
- [18] Online figure- (cited on 15th March 2011; 16:57). Available on the internet address http://www.biochem.arizona.edu/classes/bioc462/462a/NOTES/Nucleic_Acids/nucacid_structure.html
- [19] J. Lipfert, D.A. Koster, I.D. Vilfan, S. Hage, N.H. Dekker; Single-Molecule Magnetic Tweezers Studies of Type IB Topoisomerase [Online]. (cited on 17th March 2011; 9:48). Available on the internet address http://www.springerprotocols.com/Abstract/doi/10.1007/978-1-60761-340-4_7
- [20] D.W. Ussery; DNA Denaturation [Online], (cited on 22nd March 2011, 11:29): Available on the internet address http://genome.cbs.dtu.dk/staff/dave/genomics_course/2001_DNAdenature.pdf

Figures

Figures 1, 4, 14 taken from [4]

Figure 2 taken from [1]

Figure 3 taken from [5]

Figure 5, 6, 7 and 8 taken from [6]

Figure 9 taken from [14]

Figure 10 taken from [7]

Figure 11 taken from [18]

Figure 12, 13 taken from [2]

Figure 15 taken from [11]